

Local physics of magnetization plateaux in the Shastry-Sutherland model

L. Isaev¹, G. Ortiz¹, and J. Dukelsky²

¹*Department of Physics, Indiana University, Bloomington IN 47405, USA*

²*Instituto de Estructura de la Materia - CSIC, Serrano 123, 28006 Madrid, Spain*

We address the physical mechanism responsible for the emergence of magnetization plateaux in the Shastry-Sutherland model. By using a hierarchical mean-field approach we demonstrate that a plateau is stabilized in a certain *spin pattern*, satisfying *local* commensurability conditions derived from our formalism. Our results provide evidence in favor of a robust local physics nature of the plateaux states, and are in agreement with recent NMR experiments on $\text{SrCu}_2(\text{BO}_3)_2$.

PACS numbers: 75.10.Jm, 75.60.Ej

Introduction.— The interplay between quantum mechanics and the atomic lattice topology often leads to a complex mosaic of physical phenomena in low-dimensional frustrated magnets [1]. A prominent representative of this class of materials is the layered compound $\text{SrCu}_2(\text{BO}_3)_2$, which recently received a lot of attention because of its fascinating properties in an external magnetic field h , namely the emergence of magnetic plateaux at certain fractions of the saturated magnetization M_{sat} . The first experimental observations of the plateaux were reported in [2] for $m = M/M_{\text{sat}} = 1/8$ and $1/4$, and somewhat later for $m = 1/3$ [3]. Subsequent nuclear magnetic resonance (NMR) experiments [4, 5] revealed spontaneous breaking of the lattice translational symmetry within the $1/8$ plateau, and also indicated that the spin superlattice persists right above this fraction [6]. The field was reignited by the work of Sebastian et al. [7], where additional plateaux at exotic values $m = 1/9, 1/7, 1/5$ and $2/9$ were reported. However, direct observation of the emerging spin superstructures remains an experimental challenge, primarily due to the high magnetic fields ($\sim 30 - 50$ Tesla) involved in measurements.

The nature of the magnetic states and physical mechanism leading to the plateaux are also yet to be understood. It is believed that the Heisenberg antiferromagnetic model on a frustrated Shastry-Sutherland (SS) lattice with N sites [8] (Fig. 1),

$$H = J \sum_{\langle ij \rangle} \mathbf{S}_i \cdot \mathbf{S}_j + 2J\alpha \sum_{[ij]} \mathbf{S}_i \cdot \mathbf{S}_j - h \sum_i S_i^z, \quad (1)$$

captures the essential magnetic properties of $\text{SrCu}_2(\text{BO}_3)_2$ in relatively high fields. In Eq. (1) \mathbf{S}_i denotes a spin-1/2 operator at site i ; the first sum is the usual nearest-neighbor (NN) Heisenberg term, while the second one runs over dimers; J and $\alpha \geq 0$. This model is quasi-exactly solvable [8] for $\alpha \geq 1 + h/2$: the ground state (GS) is a direct product of singlet dimer states, and was shown to be stable up to $\alpha \sim 0.71-0.75$ in zero field [9]. In general, it is an intractable quantum many-body problem where approximation schemes are needed to deal with large- N systems.

All theories proposed to address this unusual magne-

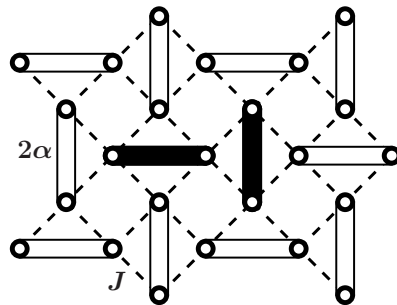


FIG. 1: The SS lattice. Circles denote spins, dashed lines correspond to the NN J coupling, double solid lines denote next-NN interactions (dimers). The simplest choice of a degree of freedom, which does not cut dimers, is shown in black.

tization phenomenon start from the SS model. However, the physical mechanism stabilizing the plateau states, their nature, and the structure of the magnetization curve are still actively debated. Current ideas can be broadly divided into two groups. The first one advocates subtle non-local (in the spins) correlations leading to an underlying spin structure which preserves lattice symmetries [10]. Technically, it employs a mapping of the original spins to fermions coupled to a Chern-Simons gauge field, and then performs a Hartree-Fock decoupling. In this way, the qualitative shape of the $\text{SrCu}_2(\text{BO}_3)_2$ magnetization curve was reproduced in high fields, but the lowest plateau at $1/8$ was missing. Later, this non-local mean-field approach was extended to include inhomogeneous phases [7], and it was argued that the plateaux correspond to stripe states with broken lattice symmetries. Remarkably, the length scale ξ associated with the emerging spin superlattice was found to be $\xi \sim 100$ lattice spacings. The second group contends that the magnetization process can be described in terms of polarized dimers (triplons), which propagate in the background of singlet dimers [9, 11]. They developed effective hardcore boson models (truncating the original dimer Hilbert space), solved by perturbative [12] or CORE [13] techniques, and found that the plateaux states correspond to crystal phases with $\xi \sim 10$ lattice constants.

Such diversity of theoretical predictions demands further investigation. In this paper we use the hierarchical mean-field (HMF) method [14], in an attempt to clarify the nature and physical mechanism, responsible for the emergence of magnetic plateaux in the SS model. Unlike previous calculations, we deal directly with the SS Hamiltonian (1), not with effective Hamiltonians as in Refs. [12, 13], and combine exact diagonalization data with a simple and *controlled* approximation for the GS wavefunction. For instance, we do not discard the $M = 0$ dimer triplet states, necessary for the propagation of a triplon. We focus on higher-lying fractions, whose existence has been confirmed experimentally. Our results support the *local* physics nature of the plateau states. In particular, it is explicitly demonstrated how to construct those robust states based on a set of commensurability rules that we derived. Our conclusions are also in agreement with the interpretation of NMR measurements [4].

Method.— The HMF approach is based on the assumption that the physics of the problem is *local* in a particular representation. Since the SS model is formulated in terms of localized spins, it is natural to work in real space. The main idea of our method revolves around the concept of a *relevant* degree of freedom – a spin cluster – which is used to build up the system. Essential quantum correlations, which drive the physics of the problem, are captured by this local representation. The SS Hamiltonian is then rewritten in terms of these coarse-grained variables and a mean-field decoupling is eventually applied to determine properties of the system. The method is only limited by finite-size effects and becomes asymptotically exact in the thermodynamic limit. Thus, the (generally) exponentially hard problem of determining the GS of the model is reduced to a *polynomially* complex one. By identifying each state of a cluster with a Schwinger boson (SB) and computing matrix elements of spin operators between these states, one can rewrite *exactly* the Hamiltonian of Eq. (1) in terms of new (cluster) variables

$$H = \sum_i \epsilon_a(\alpha, h) \gamma_{ia}^\dagger \gamma_{ia} + \sum_{\langle ij \rangle_\sigma} (H_{\text{int}}^\sigma)_{ab}^{a'b'} \gamma_{ia}^\dagger \gamma_{jb'}^\dagger \gamma_{ia} \gamma_{jb}. \quad (2)$$

Here the repeated indices a , b , etc., which label states of an N_q -spin cluster, are summed over, and i denotes sites in the coarse-grained lattice. The operators γ_{ia}^\dagger that create a particular state of a cluster are $SU(2^{N_q})$ SBs subject to the constraint $\sum_a \gamma_{ia}^\dagger \gamma_{ia} = 1$ on each site; ϵ_a are exact cluster eigenenergies. Since the original SS Hamiltonian involves only two-spin interactions, in the new representation there will be only two-boson scattering processes: the corresponding matrix elements are denoted by $(H_{\text{int}}^\sigma)_{ab}^{a'b'}$. The second term in Eq. (2) describes the renormalization of the cluster energy due to its interaction with environment. Thus, our method deals with an infinite system and finite-size effects enter

only through a particular choice of the cluster. The symbol $\langle ij \rangle_\sigma$, with $\sigma = 1, 2, \dots$, indicates pairs of neighboring blocks, coupled by the same number of J -links.

Application of the HMF method to the SS model starts by recalling that the phases within plateaux break the lattice translational invariance. Therefore, the best solution will be obtained, if the degree of freedom matches the unit cell of the spin superstructure. For each cluster size, N_q , and magnetization

$$m = \frac{1}{M_{\text{sat}}} \sum_i \langle S_i^z \rangle = \frac{2}{N} \sum_i \langle S_i^z \rangle = \frac{2}{N_q} \sum_{j=1}^{N_q} \langle S_j^z \rangle,$$

we determine the lowest-energy configuration (i.e., the cluster shape and corresponding tiling of the lattice). By virtue of previous argument, this solution will have the “right” symmetry. Performing this operation for successive values of N_q up to the largest one that can be handled, we obtain a set of magnetization plateaux together with their corresponding spin profiles. It follows that the particular choice of coarse graining is critical for the success of this program. One should recall that the experimental value for α is 0.74-0.84, i.e. the intradimer coupling seems to be “more relevant” than the interdimer one. Therefore, it is natural to consider only those clusters, which contain an integer number of α -links. This constraint turns out to be quite severe. It follows that the degree of freedom must also contain an integer number of “minimal” blocks, shown in Fig. 1 in black: otherwise the tiling of the lattice will not be complete. These requirements comprise a set of local commensurability conditions, necessary to stabilize a plateau.

Another crucial issue is the way the interaction terms in Eq. (2) are handled. In an attempt to simplify matters, we use the straightforward Hartree approximation, i.e., we consider the trial GS wavefunction

$$|\psi_0\rangle = \prod_i (R_a \gamma_{ia}^\dagger) |0\rangle; \quad R_a^* R_a = 1. \quad (3)$$

Here $|0\rangle$ is the SB vacuum and R_a are variational parameters, which constitute the cluster wavefunction. Since H is real-valued, we can choose R_a to be also real. Clearly, this state is cluster translationally invariant and has exactly one boson per coarse-grained lattice site (so the constraint is exactly satisfied). Next, we compute the expectation value of H in the state (3), subject to periodic boundary conditions, and minimize it with respect to R_a . In this manner one obtains the approximate GS energy E_0 as a function of the magnetic field h .

It is important to emphasize the simplicity of our approach. By using a more sophisticated ansatz (e.g. a Jastrow-type correlated wavefunction [14]), we could improve energies but the physical mechanism and robust structure of the plateaux will remain intact. Despite its simplicity, the ansatz of Eq. (3) was accurate enough to

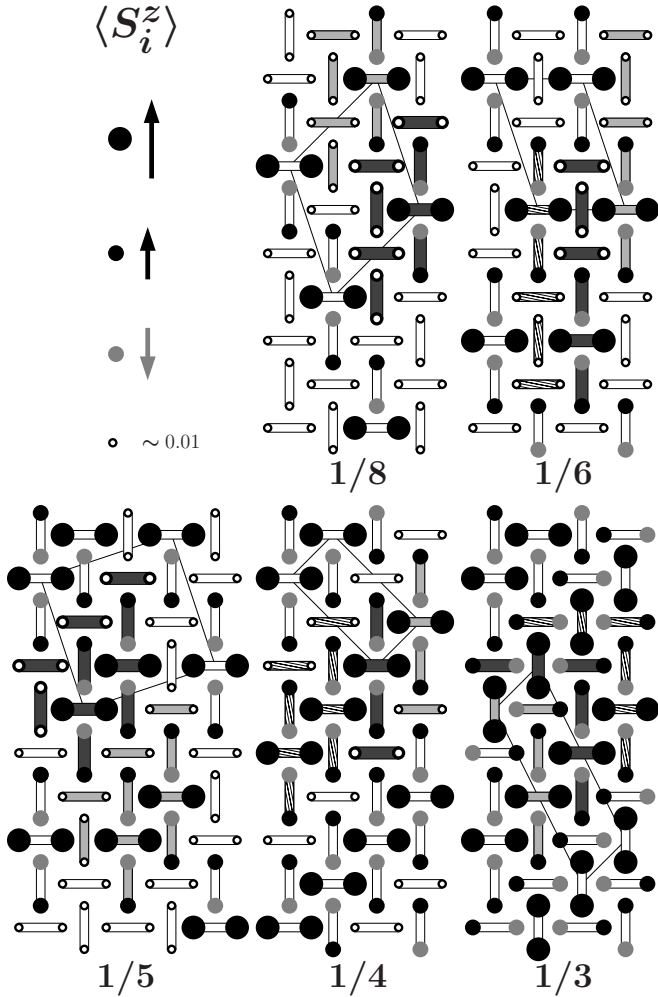


FIG. 2: Schematic spin profiles within plateaux. (Gray) black circles correspond to polarizations (anti) parallel to the field; their sizes encode the magnitude of the local magnetic moment. Empty circles denote sites with $|\langle S_i^z \rangle| \lesssim 10^{-2}$. The clusters used in HMF calculations consist of dark gray dimers. Light gray dimers represent the NN cluster. For $m = 1/3, 1/4$ and $1/6$ dark and hatched dimers constitute the 24-spin cluster. Thin lines indicate unit cells of the spin superlattice.

yield the quantitatively correct phase diagram of the J_1 - J_2 model [14], which involves gapless phases. In the SS model states within the plateaux are gapped, therefore, our method should be tailored for this problem.

Results.— To guarantee that our results reduce to the exact solution in the limit $h \rightarrow 0$, we mainly consider the region $\alpha \gtrsim 1$. The simplest degree of freedom, consisting of 4 spins, is shown in Fig. 1. Using this cluster in our HMF scheme one obtains stable plateaux only at $m = 1/2$ and $m = 1$. Clearly, larger blocks are necessary to stabilize plateaux at lower magnetization fractions. Here, we consider cluster sizes $N_q = 4k$ with $k = 2, \dots, 6$ and discuss only plateaux at $1/3, 1/4, 1/5, 1/6$ and $1/8$, supported in minimal clusters of $N_q = 12$,

TABLE I: Representative values of the GS energy parameter ε_0 . Numbers in parenthesis denote the size of a cluster, N_q .

α	1/8	1/6	1/5	1/4	1/3
1.1	0.72056	0.68561 (24)	0.65678	0.61291 (24)	0.53553 (24)
		0.68318 (12)		0.61121 (16)	0.53212 (12)
2.0	1.26734	1.18978 (24)	1.12758	1.03384 (24)	0.87689 (24)
		1.18937 (12)		1.03336 (16)	0.87569 (12)

8, 20, 12 and 16 spins, respectively ($M_{\text{sat}} = N_q/2$). In Fig. 2 we present local spin profiles, corresponding to the lowest energy configurations, for each of these fractions. Comparison of patterns for different plateaux, shows that states $1/n$ with n even are characterized by one polarized dimer per unit cell, while cells of odd- n states have two triplons. For a given plateau, there typically exist several possible coarse-graining scenarios, characterized by different clusters and tessellations of the SS lattice, but identical unit cells. Although these configurations have slightly different energies, their existence provides an important check for robustness of local correlations, stabilizing the plateau states. The patterns for all fractions except $1/5$, are similar to those obtained in Refs. [4, 12]. Strictly speaking, the profiles in Fig. 2 are well defined only for large values of $\alpha > 1$ and quickly smear out with decreasing α . This effect is difficult to capture within the effective model calculations, like [12].

A clear advantage of our approach, compared to previous works, is its ability to compute GS energies of the *original* SS model. Within each plateau we have: $E_0(h)/N = -\varepsilon_0 - mh/2$. The parameter ε_0 is presented in Table I for some values of α and different cluster sizes. In order to address finite-size effects, in Fig. 3 we present the high magnetic field phase diagram of the SS model for $\alpha \geq 1$. All fractions were calculated using the largest possible cluster. Due to the insulating nature of the plateau states, the finite-size corrections are not expected to significantly affect their stability. For instance, for $m = 1/6$ the energy difference between 12- and 24-spin clusters is only $\sim 5\%$ of its width for the values of α shown in Table I. This observation serves as additional evidence in favor of a universal physical mechanism leading to the plateaux.

As it was already mentioned, the HMF method does not involve truncation of the dimer Hilbert space. In order to understand consequences of this approximation, we computed ε_0 for different plateaux, ignoring the dimer state $|\downarrow\downarrow\rangle$. The resulting absolute error is of the same order of magnitude as finite size effects and plateau widths (cf. Table I), which leads to a sizable change in the relative stability of the plateaux. For example, at $\alpha = 1.1$ the average error is $3 \cdot 10^{-3}J$, and the lower boundary of the $1/8$ state shifts by $0.04J$. Therefore, conclusions of the effective boson model calculations, which employ similar truncation, should generally be taken with caution.

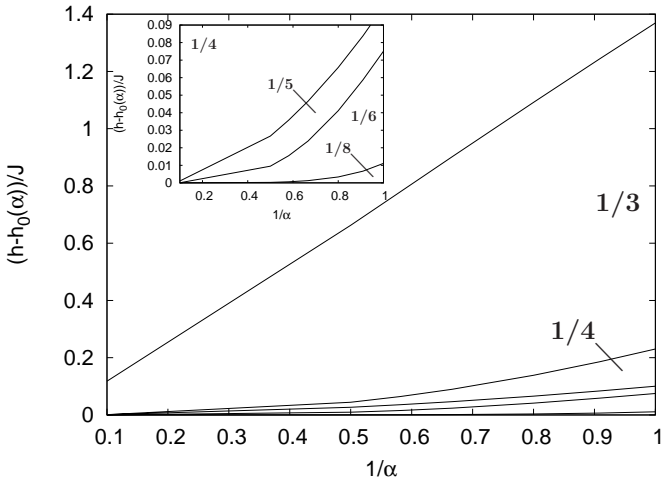


FIG. 3: High magnetic field phase diagram of the SS model for $\alpha \geq 1$. $h_0(\alpha)$ denotes the field after which the first plateau (at 1/8) emerges. Fractions indicate values of m . For $\alpha \gg 1$ the triplons (●—●) in Fig. 2 become fully polarized and other dimers within the clusters turn into perfect singlets.

Discussion.— Although the effective model approach does yield a sequence of plateaux, their understanding remains incomplete. Our work addresses this issue by focusing on the nature and correlations of the magnetic plateau states. In particular, the analysis presented above, allows the formulation of a set of *universal* rules leading to well-defined *spin patterns* (Fig. 2), which can be probed, e.g. by neutrons. These rules define a hierarchy of variational plateau wavefunctions and constitute a central prediction of our work. For a robust state to emerge at a given magnetization fraction m , the *commensurability conditions* that have to be fulfilled are: (i) the (cluster) degree of freedom must contain an even number of dimers; (ii) the SS lattice must be tessellated completely with these clusters; (iii) the size of the cluster (unit cell), N_q , must allow the plateau state at m , therefore, $N_q = 2M/m$ with $M = 1, \dots, N_q/2$ chosen in a way such that N_q is divisible by four; (iv) the number of triplons (●—●) per cluster is M and its shape must be such that each triplon is surrounded by two dimers of the type ●—●, within this cluster. The application of the above constraints leaves us with the essentially combinatorial problem of actually determining the symmetry and periodicity of the spin superstructure (see Fig. 2).

There also exists a number of concrete discrepancies between our work and recent publications [12, 13], which, nevertheless, support our general conclusion regarding the local nature of the plateau states. First, the experimentally observed plateaux at 1/4 and 1/8, which we found to be quite robust, were claimed to be unstable in [12]. However, the magnetization profile, presented in Fig. 2 for $m = 1/8$, which persists at $\alpha = 0.787$, adequate for $\text{SrCu}_2(\text{BO}_3)_2$, is consistent with the interpretation of

available NMR data [4, 5] for this material. We believe that the origin of these states is purely magnetic and no additional interactions beyond the SS model are required, in contradiction with the claim of Ref. [12]. Our results also yield a stable 1/5 plateau, contrary to the conclusions of Refs. [12, 13]. We note that this fraction was observed in torque measurements of [7], however, their proposed spin superlattice differs dramatically from the one predicted in our Fig. 2. Another distinction concerns the robustness of the 1/6 plateau advocated in [12], which, although present in our calculation, has a significantly smaller relative width (see the discussion above). Other fractions at 1/9, 2/9 and 2/15, observed in Refs. [12] and [13], can also be obtained within our approach, but this requires significantly larger clusters than the ones used here. By virtue of our commensurability arguments, we expect the plateaux at 1/9 and 2/9 to emerge in degrees of freedom containing at least 36 spins, while the 2/15 fraction will be stabilized in a 60-spin cluster.

Finally we note that the precise shape of the magnetization curve (the relative energy stability of different plateaux) is quite sensitive to the value of α (i.e., the particular compound) and, most importantly, since there is no exact solution of the SS model at these high fields, it depends on the particular approximation scheme. Experimentally, other physical interactions not included in the SS model may also add to this uncertainty.

Acknowledgements.— We thank C. D. Batista for stimulating discussions. Calculations were performed on Quarry and NTC clusters at IUB. JD acknowledges support from the Spanish DGI grant FIS2006-12783-C03-01.

- [1] J. Richter, J. Schulenburg and A. Honecker in *Quantum Magnetism*, U. Shollwöck, J. Richter, F. J. J. Farnel and R. F. Bishop eds., Springer-Verlag, Berlin 2004.
- [2] H. Kageyama *et al.*, Phys. Rev. Lett. **82**, 3168 (1999).
- [3] K. Onizuka *et al.*, J. Phys. Soc. Jpn. **69**, 1016 (2000).
- [4] K. Kodama *et al.*, Science **298**, 395 (2002).
- [5] M. Takigawa *et al.*, J. Phys. Conf. Ser. **51**, 23 (2006).
- [6] M. Takigawa *et al.*, Phys. Rev. Lett. **101**, 037202 (2008).
- [7] S. E. Sebastian *et al.*, PNAS **105**, 20157 (2008).
- [8] B. S. Shastry and B. Sutherland, Physica **108B**, 1069 (1981).
- [9] S. Miyahara and K. Ueda, J. Phys.: Cond. Mat. **15**, R327 (2003).
- [10] G. Misguich, T. Jolicoeur, and S. M. Girvin, Phys. Rev. Lett. **87**, 097203 (2001).
- [11] S. Miyahara and K. Ueda, Phys. Rev. Lett. **82**, 3701 (1999); Phys. Rev. **B61**, 3417 (2000). T. Momoi and K. Totsuka, Phys. Rev. **B62**, 15067 (2000).
- [12] J. Dorier, K. P. Schmidt, and F. Mila, Phys. Rev. Lett. **101**, 250402 (2008).
- [13] A. Abendschein and S. Capponi, Phys. Rev. Lett. **101**, 227201 (2008).
- [14] L. Isaev, G. Ortiz, and J. Dukelsky, Phys. Rev. **B79**, 024409 (2009).